Soils and Foundations 2015;55(3):614–625

HOSTED BY

ELSEVIER

CrossMark

The Japanese Geotechnical Society

Soils and Foundations

www.sciencedirect.com
journal homepage: www.elsevier.com/locate/sandf

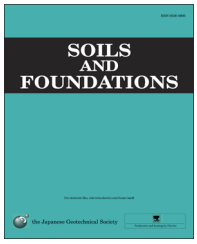

Numerical modelling of pile foundation angular distortion

Brian B. Sheil, Bryan A. McCabe*

College of Engineering and Informatics, National University of Ireland, Galway, Ireland

Received 29 November 2013; received in revised form 11 January 2015; accepted 6 February 2015
Available online 16 May 2015

Abstract

In this paper, the PLAXIS 3-D Foundation finite element (FE) software package, in conjunction with the nonlinear Hardening Soil (HS) constitutive model, is employed in an extensive parametric study of the angular distortion of piled foundations. Angular distortion has been documented as the most influential settlement characteristic in the cracking of buildings. Numerical results are appraised in the context of the acceptable limits for angular distortion, recommended in the literature and set down in geotechnical building codes, since there is currently no guidance in the literature on appropriate pile cap rigidities for remaining safely within these limits. The results of the parametric study were validated by a comparison to the measured differential settlement characteristics from buildings and full-scale pile groups documented in the literature for which a good agreement was obtained. In addition, the numerical data has been formulated into a set of fully-normalised trends. Although a relatively wide range of variables are considered in the parametric study, a consistent trend between the average settlement performance and angular distortion for corresponding pile cap rigidities was evident. These trends present design engineers with a useful resource for estimating the angular distortion of piled foundations.

1. Introduction

During the past couple of decades, a significant increase has been seen in the number of structures, particularly tall buildings, founded on piled foundations (Poulos, 2001). In parallel, the focus of foundation design has shifted from the ultimate limit state design to the serviceability limit state design, and on the serviceability front, designers are increasingly considering the differential settlements as well as the maximum settlements in a foundation system. While the maximum settlements of foundation systems have received ample treatment in the literature, differential settlements have received less attention.

Where investigations of differential settlements have been reported, they have mainly been related to piled raft foundations, e.g., Horikoshi and Randolph (1998), Prakoso and Kulhawy (2001), Reul and Randolph (2004) and Cho et al. (2012). A number of these studies have found that optimising the design of a piled raft foundation involves locating the piles near the centre of the foundation in order to minimise the total differential settlements. In addition, parametric analyses have identified the ratio of the pile group width to the pile raft width, the group size, the raft–soil stiffness ratio and the applied load configuration as having the greatest impact on differential settlements, whereas pile length has been deemed less influential.

While those studies considered the *magnitude* of differential settlements occurring across a piled raft, Skempton and MacDonald (1956) identified the radius of curvature as the most influential settlement characteristic causing the cracking of buildings. They compiled a database of 98 case histories with the goal of developing limits for the total and differential settlements of various foundations. Since the radius of curvature proved very difficult to measure accurately, they proposed

*Corresponding author.
E-mail address: bryan.mccabe@nuigalway.ie (B.A. McCabe).
Peer review under responsibility of The Japanese Geotechnical Society.

http://dx.doi.org/10.1016/j.sandf.2015.04.012

angular distortion (β) as a more practical measure of differential settlement, defined as the ratio of the differential settlement to the horizontal distance between measurement stations.

A selection of the limits for β, documented in the literature, is presented in Table 1 through observations of damage to buildings founded on both clay and fill. The limits presented by Zhang and Ng (2005) were derived from a database of the settlement characteristics of 300 buildings within a probabilistic framework. In light of these studies, there now appears to be a general consensus in the literature that angular distortion greater than 1/300 is likely to induce damage in ordinary buildings, although Eurocode 7 has recently set out a more conservative 1/500 tolerable limit. Also relevant is Rethati's (1961) observation that 91% of the damage from his database was associated with buildings of two storeys or lower and concluded that the rigidity of the supported structure should also be taken into account when considering angular distortion.

While the extent of angular distortion likely to cause building damage is now relatively well established, a considerable lack of information remains in the literature on the rigidity of piled foundations required to comply with these limits. Moreover, in cases where levels of angular distortion are relatively low, there is the potential for considerable savings in foundation construction by optimising the design of the pile cap, particularly for larger group sizes. In this paper, the PLAXIS 3-D Foundation finite element (FE) software package, in conjunction with the nonlinear Hardening Soil (HS) constitutive model, has been employed in an extensive parametric study of the angular distortion of piled foundations. Numerical results are appraised in the context of the aforementioned limits for angular distortion. In addition, results from the parametric study are validated by comparing them to measured differential settlement characteristics from buildings and full-scale pile groups documented in the literature. The numerical data is then formulated into fully-normalised trends with the intention of providing design engineers with a useful resource for estimating the angular distortion of piled foundations.

2. Details of the finite element modelling

2.1. Default HS parameters

The default HS soil parameters used in the parametric study are documented in Sheil and McCabe (2014). E_{oed} was determined from oedometer tests, while E_{50} and E_{ur} were determined from triaxial compression tests in primary loading and unloading/reloading, respectively. In addition, parameter m was determined by curve-fitting to the stress-strain curve in triaxial compression. It has already been shown by Sheil and McCabe (2014) that these parameters represent the behaviour of a soft clay/silt site in Belfast, Northern Ireland and predict the load-displacement behaviour of a single pile and a 5-pile group in this clay/silt (McCabe and Lehane, 2006) very well. In addition, these parameters were used to arrive at a finite element-based empirical approach for the prediction of pile group settlement performance which compared well to a database of case histories in a range of clay types (Sheil and McCabe, 2014). Obviously, the parametric study has necessitated variations upon some of the default parameters.

Table 1
Limits for angular distortion.

Reference	Limits
Skempton and MacDonald (1956)	$\beta < 1/300$
Rethati (1961)	
Jappeli (1965)	
Wahls (1994)	$\beta < 1/125$–$1/250$
Zhang and Ng (2005)	$\beta < 1/86 \pm 1/70$ (intolerable)
	$\beta < 1/357 \pm 1/417$ (tolerable)
Eurocode 7	$\beta < 1/500$

2.2. FE model parameters

The pile/soil parameters considered in the study are illustrated in Fig. 1. The default pile length (L) and diameter (D) are 6.0 m and 0.282 m, respectively (the diameter gives an equivalent pile area to that of a square pile of width 0.25 m). These dimensions are based on the pile sizes tested by McCabe and Lehane (2006). E_1 is the stiffness of the upper layer, E_2 is the stiffness of the lower layer and the boundary between them occurs at a depth h below ground level, where h is greater than or equal to L. In all analyses, a value of $h/L=3$ was maintained, except in Section 4.7 where $h/L=1$. The depth below ground level to the bottom mesh boundary, H, was chosen as 3 L so that the lower mesh extremity had no effect on the FE output. Likewise, the lateral boundaries of the FE model for each analysis were located at a distance such that no influence on the output was recorded.

Other features of the model are shown in Fig. 2 (the illustration is for a free-standing 16-pile group). 15-node wedge elements were used in the study comprising of 6-node triangular

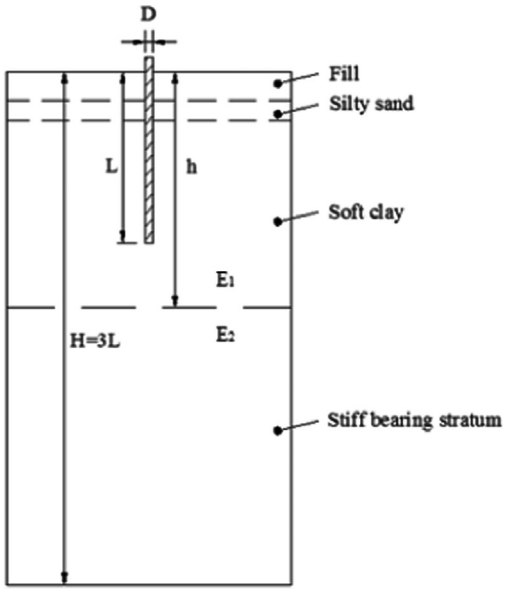

Fig. 1. Illustration of pile/soil parameters.

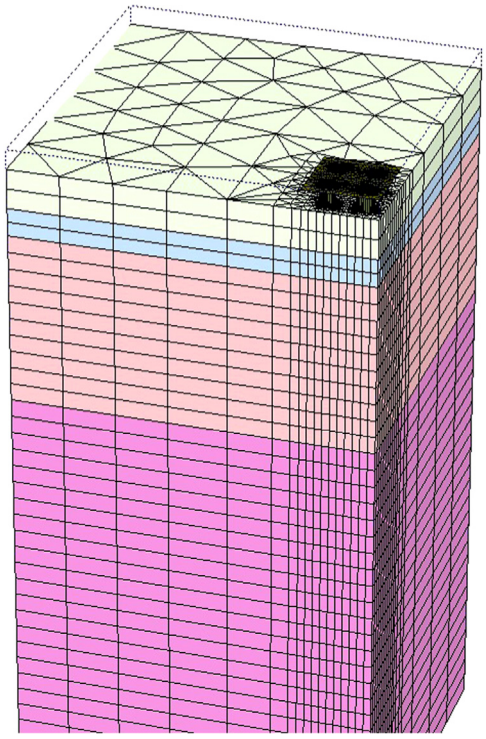

Fig. 2. Finite element mesh for free-standing 16-pile group.

elements in the horizontal direction and 8-node quadrilateral elements in the vertical direction. Symmetry was exploited to reduce the number of elements used in the mesh. In all analyses, the mesh was refined in zones of high stresses near the piles. Coarse, medium and fine meshes were used to confirm the mesh convergence for all analyses. Further details are available in Sheil and McCabe (2014).

2.3. Stages of analysis – free-standing groups

Although both piled rafts and free-standing pile groups are considered in this study, free-standing pile groups form the basis of the parametric study in Section 4. Free-standing pile foundations have served as a common means for supporting offshore platforms and wind turbines in shallow water depths, for example, Gavin et al. (2011). The stages used in the analysis of a free-standing pile group are defined as follows:

(i) Inclusion of interface elements in the soil model to allow for pile–soil slip.
(ii) Initial stress generation by the K_0 procedure, a special calculation method available in PLAXIS.
(iii) Installation of the concrete piles reflected by changing appropriate elements to a linear elastic material with a Young's modulus of 30 GPa (in compression) and a Poisson's ratio, ν, of 0.15.
(iv) Excavation of soil to a depth of 0.5 m below the pile heads. For a free-standing pile group in PLAXIS, it is necessary to excavate the soil below the pile cap so that it does not come into contact with the ground surface. To ensure that the excavation of the soil in stage (iv) does not induce changes to the initial stresses in the soil, a dummy material is introduced to a height of 0.5 m above the soil profile with weight density $\gamma = 0$ kN/m^3.
(v) Installation of the pile cap (modelled as a 'floor' in PLAXIS) along the top of the pile group. Floors in PLAXIS are composed of 6-node triangular plate elements. Both the Young's modulus and the thickness of the pile cap are varied in the parametric analyses presented later.
(vi) Pile group loading by placing a compressive uniformly-distributed load on the top surface of the pile cap, as used by Cheung et al. (1988). Reul and Randolph (2004) documented that a uniformly-distributed load is more likely to induce differential settlements of a piled raft than a loading system representative of loads transferred from exterior walls. However, in Section 4.8, pile loading applied through the columns of the framed structure is also considered; the total loading was applied over n storeys as a UDL representing an average FS in keeping with the preceding analyses.

3. Basis for parametric study

3.1. Definition of pile cap flexibility

A goal of this study is to relate angular distortion to pile cap flexibility. Various analytical expressions have been developed to describe the flexibility of a pile cap. The form for these expressions has its origin in the plate bending theory, such as the expression given in Eq. (1) (Timoshenko and Woinowsky-Krieger, 1959)

$$K_p = \frac{E_p t_p^3}{12\left(1-\nu_p^2\right)} \tag{1}$$

where K_p is the bending stiffness of a plate, E_p is the Young's modulus of the plate, t_p is the thickness of the plate and ν_p is the Poisson's ratio of the plate.

Brown (1975) provided a more appropriate expression for the rigidity of a raft by incorporating the influence of the interaction between the raft and the underlying soil, defined as follows:

$$K_r = \frac{4E_r B_r t_r^3\left(1-\nu_s^2\right)}{3\pi E_s L_r^4} \tag{2}$$

where K_r is the relative raft–soil stiffness, E_r is the Young's modulus of the raft, B_r is the width of the raft, L_r is the length of the raft, t_r is the thickness of the raft, ν_s is the Poisson's ratio of the soil and E_s is the Young's modulus of the soil.

These approaches, however, do not take into account the influence of the piles on the rigidity of the pile cap. The definition of pile cap flexibility by Cheung et al. (1988), shown in Eq. (3), has been adopted in the present study:

$$K_r = \frac{E_c t_c^3}{12\left(1-\nu_c^2\right)}\frac{w_s}{s^2 P_{ave}} \tag{3}$$

where E_c is the Young's modulus of the cap, t_c is the thickness of the cap, ν_c is the Poisson's ratio of the cap, w_s is the

settlement of a single pile under the same average load, s is the pile-to-pile spacing and P_{ave} is the average load per pile in the group. Cheung et al. (1988) reported that, in general, pile caps are designed with $\log K_r > 1$. However, the values for $\log K_r$ of a number of well-documented pile foundation case histories have been computed by the authors and were found to lie between -1.5 (Thorburn et al., 1983) and 1.5 (McCabe and Lehane, 2006). In light of this, a relatively broad spectrum of K_r values has been considered in the present study, i.e., $|\log K_r| \leq 4$, although caps with $|\log K_r| \leq 2$ are of primary interest.

3.2. Overview of parametric study

Angular distortion is defined as follows:

$$\beta = \frac{\delta}{l} \tag{4}$$

where δ is the differential settlement and l is the horizontal distance between 'measuring stations' chosen by Skempton and MacDonald (1956) as the locations of the footings supporting the building (see Fig. 3). It can also be seen from Fig. 3 that Δ denotes the maximum *differential* settlement of the footing (in this case, between stations c and e) and ρ_{max} denotes the maximum settlement of the foundation (in this case, station e experiences the greatest settlement). Therefore, the locations of the pile heads were used as the 'measuring stations' in this study.

In general, the value for β is very small and, for convenience, the inverse of β (i.e., β^{-1}) is plotted in subsequent sections and can be considered as a form of 'angular rigidity'. The values for β^{-1} presented subsequently correspond to the minimum values for each (square) group unless specified otherwise; these occurred between the corner pile and the next inner pile along the diagonal in almost all cases.

In general, a factor of safety (FS) of 1.35 on the capacity of a single pile was used as the basis of the parametric study representing the FS on unfavourable permanent loads recommended by Eurocode 7. The capacity of a single pile was defined in this study as the load required to generate a pile head displacement of 0.1 D where D is the pile diameter. The influence of the load level has also been considered in Section 4.2.

The piles in the group have been labelled alphabetically starting from the centre pile of each group and moving outwards, as shown in Fig. 4, for a 9-pile group. Thus, pile a is the centre pile for each group, while pile c, pile f, pile j and pile o are the corner piles for group sizes of 3^2, 5^2, 7^2 and 9^2 (the limiting size for this study), respectively. Also shown in Fig. 4 is the geometry of the pile cap, where B is the shortest distance between the edge of the cap and the centre of the outer piles.

3.3. Comparison to linear elastic analyses

As a validation exercise, PLAXIS output, using a linear elastic (LE) soil model, has first been compared to analytical predictions also based on LE theory (Cheung et al., 1988). A two-layered profile, having constant soil stiffness with depth (see Guo et al. (1987) for full details), is the basis of the predictions in Figs. 5 and 6. The pile–soil properties adopted in the present analyses in Figs. 5 and 6 were thus chosen to correspond to the properties adopted by those authors. In Fig. 5, the variations in P_a/P_{ave} and P_c/P_{ave} have been plotted

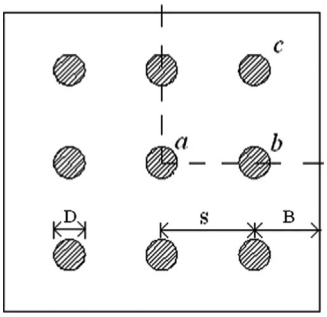

Fig. 4. Pile group geometry and labels for a 9-pile group.

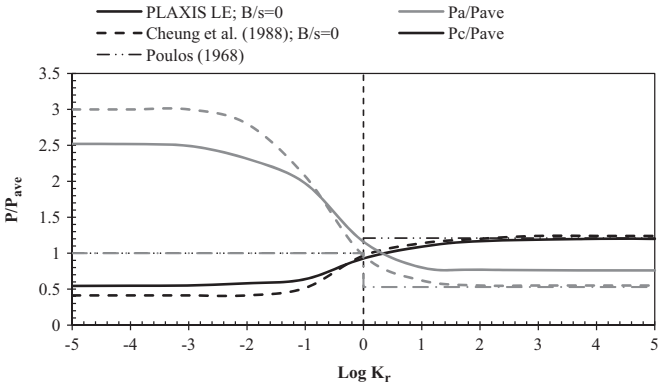

Fig. 5. Comparison of pile a and pile c load sharing to existing LE predictions; $s/D=3$, $N=9$.

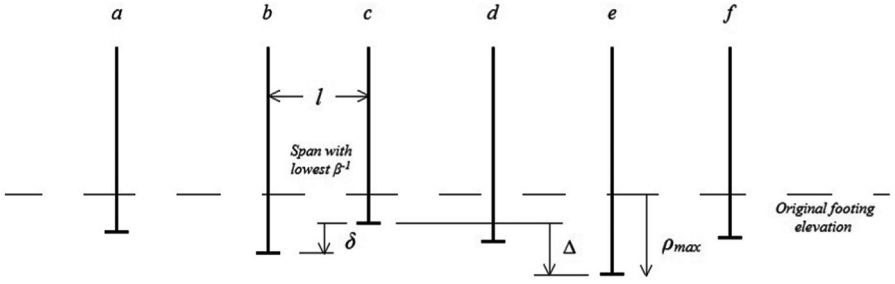

Fig. 3. Definition of settlement characteristics (adapted from Skempton and MacDonald, 1956).

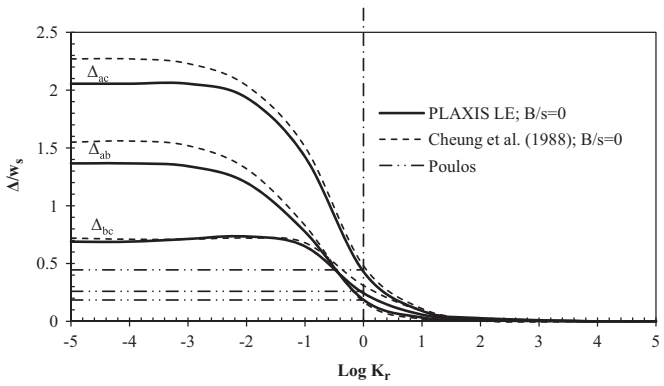

Fig. 6. Comparison of normalised differential settlement predictions; $s/D=3$, $N=9$.

versus log K_r where P_a is the load corresponding to pile a (see Fig. 4), P_c is the load corresponding to pile c and P_{ave} is the average load per pile in the group. It can be seen that the results using the LE soil model in PLAXIS agree reasonably well with the LE predictions documented by Cheung et al. (1988). While both approaches are based on the LE theory, the method by Cheung et al. (1988) does not consider the cap–pile–soil continuum directly; this contributes to some of the differences in the curves. Present predictions support the findings of Cheung et al. (1988) in which pile groups with a flexible pile cap (log $K_r \leq$ -2) do not necessarily impose an equal load on all piles.

In Fig. 6, normalised differential settlement Δ_{xy}/w_s has been plotted versus log K_r for the same analyses where Δ_{xy} is the differential settlement between pile x and pile y in the group. It can again be seen that the results using the LE soil model in PLAXIS agree well with the results by Cheung et al. (1988). It is also notable, however, that the method of interaction factors can significantly under-estimate the differential settlement of flexible pile groups due to the assumption of equivalent pile head loads. Interestingly, the predictions for the flexible pile group settlement documented by Poulos (1968) may still provide a suitable upper-bound estimate for higher pile cap rigidities (log $K_r \geq 0$).

3.4. Adopted pile cap conditions

As mentioned previously, the majority of studies that have investigated the differential settlement of piled foundations have considered piled rafts, whereas the contribution provided by cap-soil interaction has received much less attention. In Fig. 7, the variation in β^{-1} of a free-standing group has been compared to a similar group where the cap is in contact with the soil surface (i.e., a piled raft). Similar stages to those set down in Section 2.3 were used for the analysis of a piled raft, although the dummy layer was not required, and thus, was not included in the model; all other model parameters were similar. In addition, the same average load per pile was applied to the piled raft as was applied to the free-standing group (i.e., FS = 1.35 on single pile capacity).

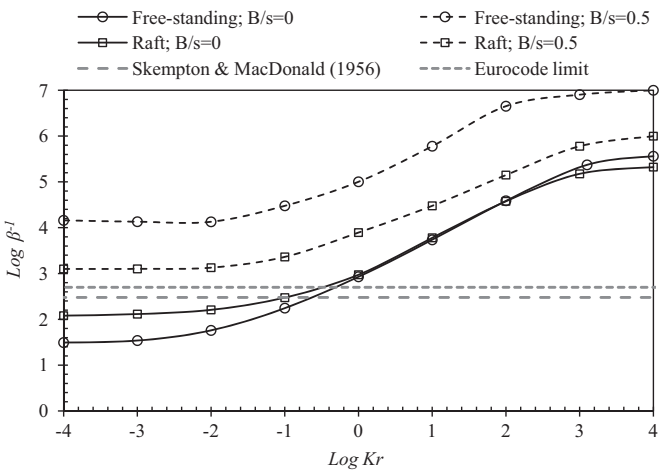

Fig. 7. Influence of cap–soil interaction and cap geometry on β^{-1}.

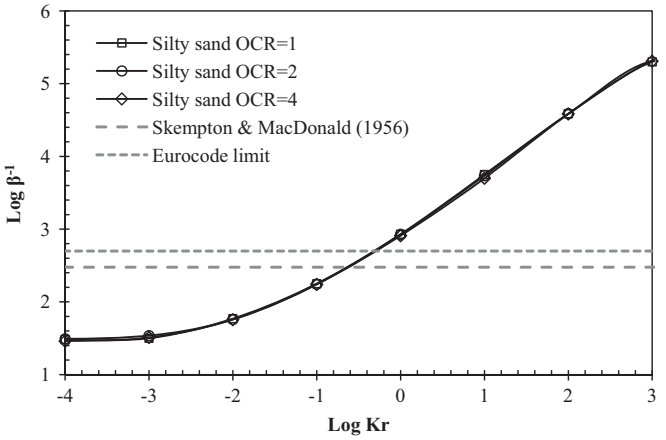

Fig. 8. Influence of silty sand OCR on β^{-1}; $N=9$, $s/D=3$.

From Fig. 7, the cap-soil interaction is found to have surprisingly little influence on the value of β^{-1} required by Eurocode 7 for a value of $B/s=0$. It can be seen that increasing the value of B/s from 0 to 0.5 has a significant influence on β^{-1} where the curves for the two foundation types diverge significantly. From these findings, it is clear that a value of $B/s=0.5$ is more appropriate for maintaining acceptable values for β^{-1}, particularly for free-standing pile groups. Since there is little guidance in the literature on commonly-employed cap over-hang distances, the authors henceforth adopt a free-standing pile group in conjunction with a value of $B/s=0$ in order to err on the side of conservatism. This is also in keeping with the modelling of Cheung et al. (1988).

3.5. Influence of adopted soil profile

Due to the uncertainty inherent in the selection of OCR for sandy soils, the OCR of the silty sand (see Sheil and McCabe, 2014) has been varied from a value of 1 to 4 in Fig. 8. It can be seen that for the adopted profile, the assumed values for OCR have a negligible influence on the PLAXIS output, largely due to the relatively small layer thickness.

In addition, to confirm that the findings of the present study are not unique to the particular soil properties adopted, the results determined using a completely different soil profile have been presented in Fig. 9. The analyses are based upon the HS parameters of the well-documented Boston Blue Clay (BBC; see McCabe and Sheil, in press) and have been compared to previous results using parameters based on the Belfast site. It is clear that while the soil type has a minor influence on β^{-1}, the difference is consistent over the spectrum of K_r values considered.

4. Parametric study

4.1. Influence of constitutive model

The influence of the stress-dependency of soil stiffness has been investigated in Fig. 10 in which the results using the HS model in PLAXIS have been compared to the results determined using the LE soil model with a constant vertical stiffness profile. The properties used for the HS model here, and henceforth in the paper, are those documented in Sheil and McCabe (2014). The properties of the LE soil model were chosen based on the equivalent small-strain stiffness values of the HS properties calibrated using the initial stiffness of the single pile load-displacement response (more details are also given in Sheil and McCabe, 2014).

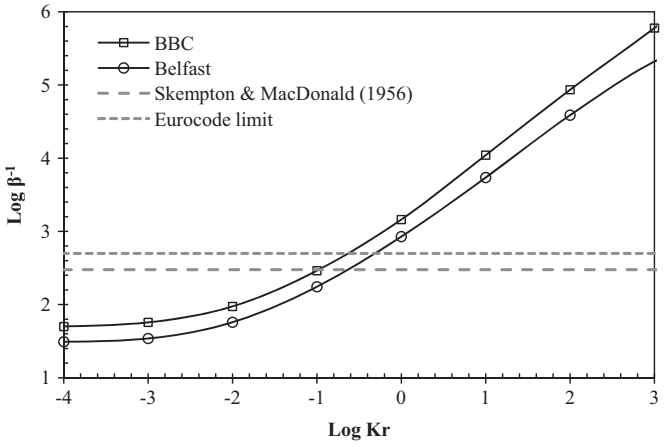

Fig. 9. Influence of soil profile on β^{-1}; $N=9$, $s/D=3$.

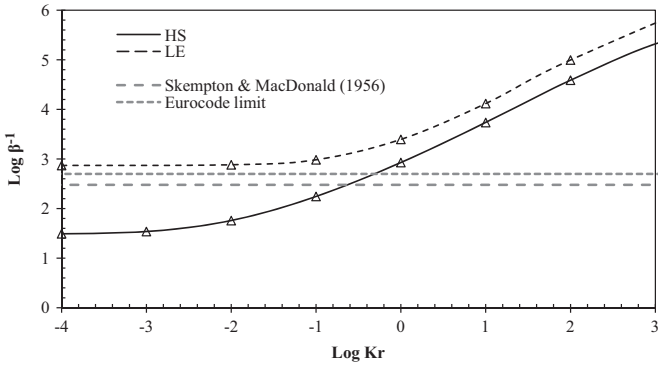

Fig. 10. Influence of soil nonlinearity on β^{-1}; $N=9$, $s/D=3$.

In Figs. 10, β^{-1} has been plotted against log K_r using both soil models. The minimum value for β^{-1} was calculated between the corner pile and next inner pile (i.e., pile c and pile a, respectively, for a group with $N=9$). It is clear that the consideration of soil nonlinearity has a significant influence on β^{-1}. A number of studies have testified to the validity of the LE analysis in pile group designs and the load test interpretation in appropriate situations, such as displacement interaction between adjacent piles, e.g., Mandolini et al. (2005) and Leung et al. (2010). However, this study shows that LE analyses provide non-conservative predictions for β^{-1}.

4.2. Influence of load level

In Fig. 11a, the influence of the load level on β^{-1} has been investigated. The results obtained using an FS of 2.5, representing a more traditional FS for pile groups (Sheil and McCabe, 2014), have been compared to the nonlinear results presented in the previous section (where a value of FS = 1.35 was used). In order to remain within the acceptable limits set down by Eurocode 7, values for log K_r of approx. -1 and 0 are required for FS values of 2.5 and 1.35, respectively. For the purpose of examining the contribution of soil nonlinearity to these differences, load-transfer curves are plotted in Fig. 11b at depths within the fill, the silty sand and the sleech layers. It can be seen that for a FOS = 1.35, significant nonlinearity is evident in the load-transfer response. It is obvious, therefore, that an underestimation of the load level experienced by a piled foundation also leads to non-conservative predictions for β^{-1}.

4.3. Influence of N

To investigate the effect of increasing the size of the group, N, predictions determined for 3^2, 5^2 and 9^2 groups have been compared in this section. Intuitively, an increase in N causes a reduction in β^{-1}, as shown in Fig. 12. The required values for log K_r to remain within the acceptable limits set down in the Eurocodes for 3^2 pile and 9^2 pile groups are significantly different.

In addition, a cross-section through the groups (see Fig. 13) was taken to investigate the distribution of β^{-1} throughout the three group sizes. In Fig. 14, an example of the distribution of β^{-1} has been plotted against the location (i.e., pile a through pile o) within the group for a value of log K_r equal to 2. The distribution confirms that the minimum values for β^{-1} occurred between the corner and next inner pile for each group size.

4.4. Influence of s/D

The influence of the pile spacing-to-diameter (s/D) on the settlement performance of piled foundations has been widely investigated in the literature. Its influence on β^{-1} is investigated in Fig. 15 by varying the value for s/D from 2 to 5 for a 9-pile group. It is clear that a reduction in s/D has an adverse

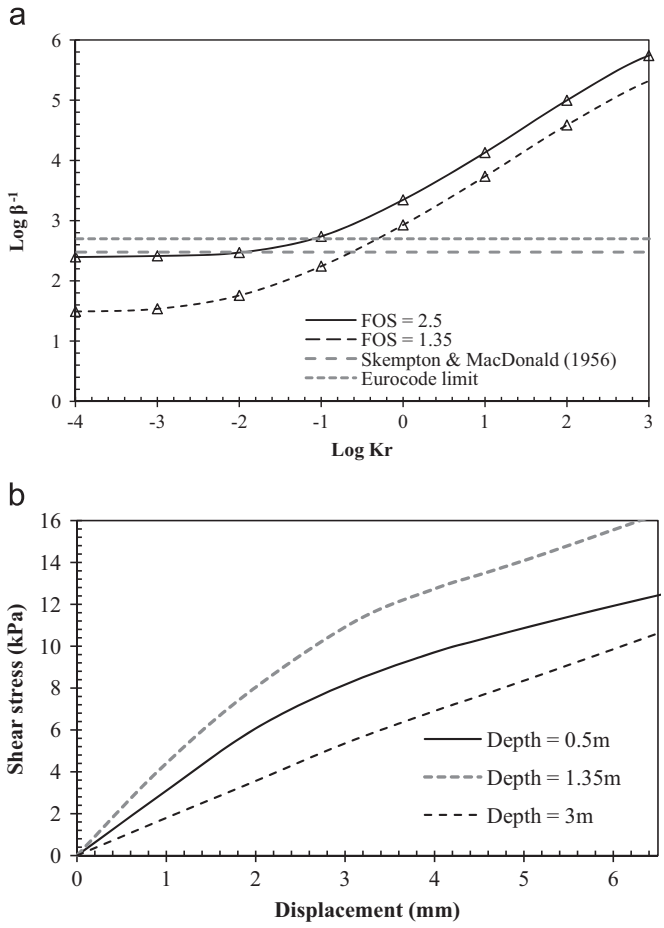

Fig. 11. (a) Influence of load level on β^{-1}; $N=9$, $s/D=3$. (b) Load-transfer curves for centre pile with FOS=1.35; log $K_r=0$, $N=9$, $s/D=3$.

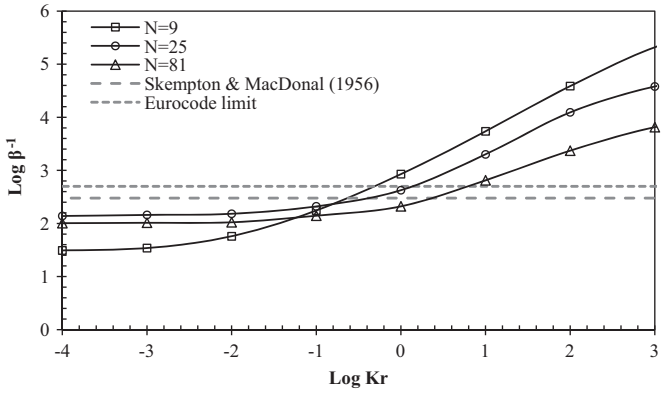

Fig. 12. Influence of group size on β^{-1}; $s/D=3$.

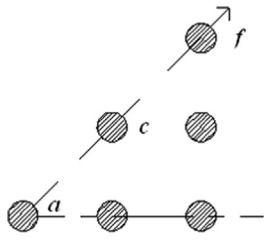

Fig. 13. Direction of cross-section taken through groups.

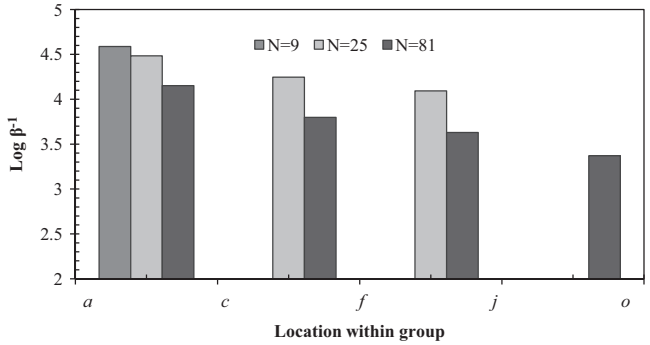

Fig. 14. Distribution of β^{-1} for log $K_r=2$.

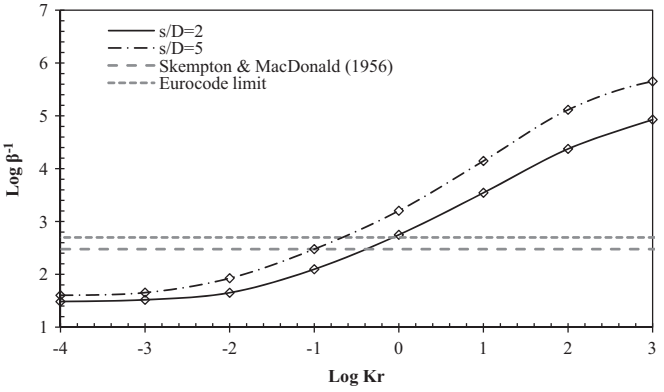

Fig. 15. Influence of s/D on β^{-1} for $N=9$.

effect on β^{-1}, to the point where the corresponding values for log K_r, needed for compliance with the Eurocode limit, differ by almost an order of magnitude. In addition, the authors have verified that there is an unique solution for a particular value of s/D, i.e., similar results for β^{-1} were observed for a group with $D=0.3$ m ($s=0.9$ m) and $D=0.6$ m ($s=1.8$ m).

4.5. Influence of group configuration

The influence of group geometry has also been taken into account where the value of m/n has been varied between 1 and 9; m and n are defined in Fig. 16. The locations of the minimum values for β^{-1} for the different group configurations were not obvious when $m \neq n$; and thus, pile cap deformation contours were used for this purpose. Fig. 17 depicts the contours for a cap with $m/n=2$ (quarter-symmetry); it can be seen that the contours become closer near the corner of the pile cap indicating the location of the minimum value for β^{-1}.

From Fig. 18, it is seen that an increase in the value of m/n surprisingly does not have an influence on the required cap rigidity recommended by Eurocode 7. Square groups (i.e., $m/n=1$) appear to exhibit a broader range of angular rigidities, while oblong configurations reach lower maximum values for β^{-1} with an increasing m/n.

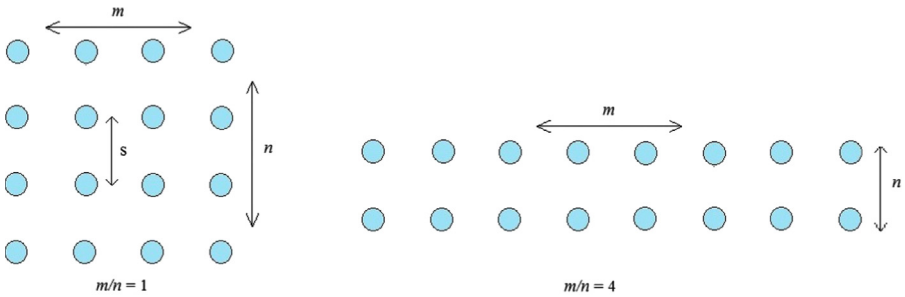

Fig. 16. Definition of *m*/*n*.

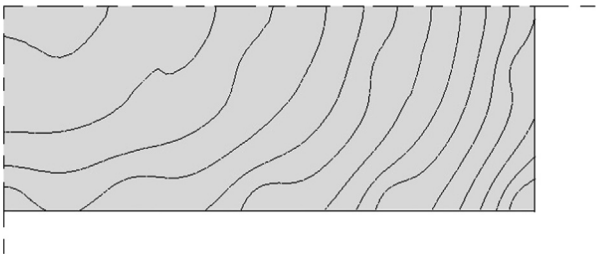

Fig. 17. Pile cap deformation contours; log K_r=0, *m*/*n*=2, *N*=36.

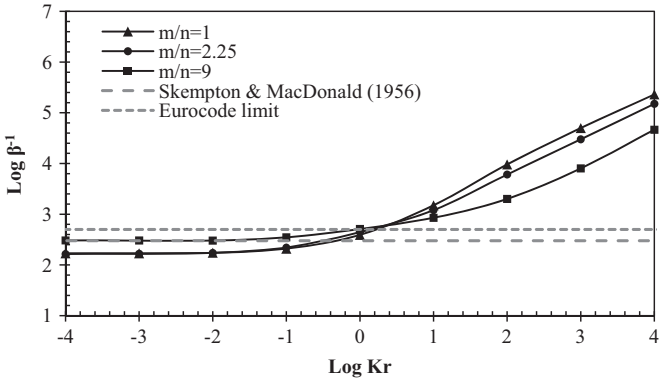

Fig. 18. Influence of group configuration on β^{-1}; *N*=36, *s*/*D*=3.

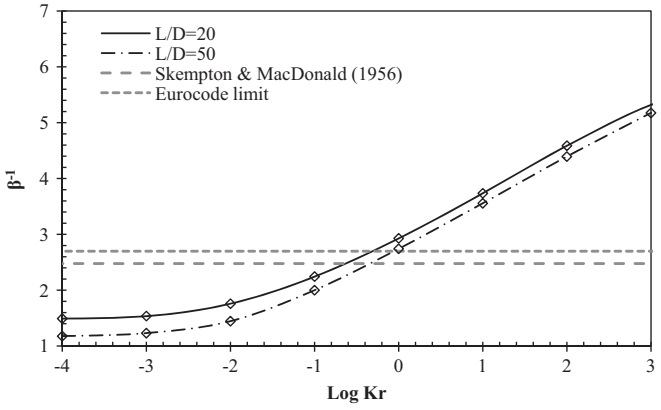

Fig. 19. Influence of *L*/*D* on β^{-1}; *N*=9, *s*/*D*=3.

4.6. Influence of L/D

The influence of pile slenderness was investigated by varying the diameter of the piles while maintaining a value of *s*/*D*=3. In Fig. 19, the variation in β^{-1} has been plotted for values of *L*/*D* equal to 20 and 50. In the course of this study, it was verified that the bending moments induced by the axial loads are smaller than the yield moment, *M*, of the pile calculated as

$$M = f_p.z \tag{5}$$

where f_p is the yield stress of the pile material (conservatively chosen as 30 MPa, i.e., mass concrete) and *z* is the elastic section modulus. In comparison to the influence of the parameters considered previously, it can be seen that the increase in *L*/*D* corresponds to a marginal reduction in β^{-1}.

4.7. Influence of E_2/E_1

For the purpose of investigating the influence of varying E_2/E_1, a stiff bearing stratum has been included in the soil model for which a value of *h*/*L*=1 has been adopted. The soil properties of the stiff bearing stratum are identical to those adopted for the soft clay, except that the soil stiffness parameters have been multiplied by a factor of E_2/E_1 similar to a previous study conducted by the authors (McCabe and Sheil, in press). Figs. 20a and b present the results of these analyses for values of E_2/E_1 ranging from 1 to 30 for *N*=9 and *N*=81, respectively. As expected, an increase in the stiffness of the bearing stratum at the base of the piles increases the angular rigidity of the group to the point where both group sizes, founded on a stratum with E_2/E_1=30, have angular rigidity that is acceptable according to Eurocode 7, regardless of the stiffness of the pile cap, although it is recognised that this is also dependent on the value adopted for *L*/*D*. From these results, it is clear that piled foundations founded on stiffer stratum have a significant scope for refining the design of pile caps.

4.8. Influence of the supported superstructure

Rethati (1961) noted that the influence of the rigidity of the supported superstructure should be taken into account when considering the angular distortion of a piled foundation. However, Grant et al. (1974) documented little influence of

the number of storeys and width of a building on the ratio of the maximum angular distortion to the maximum settlement of the building.

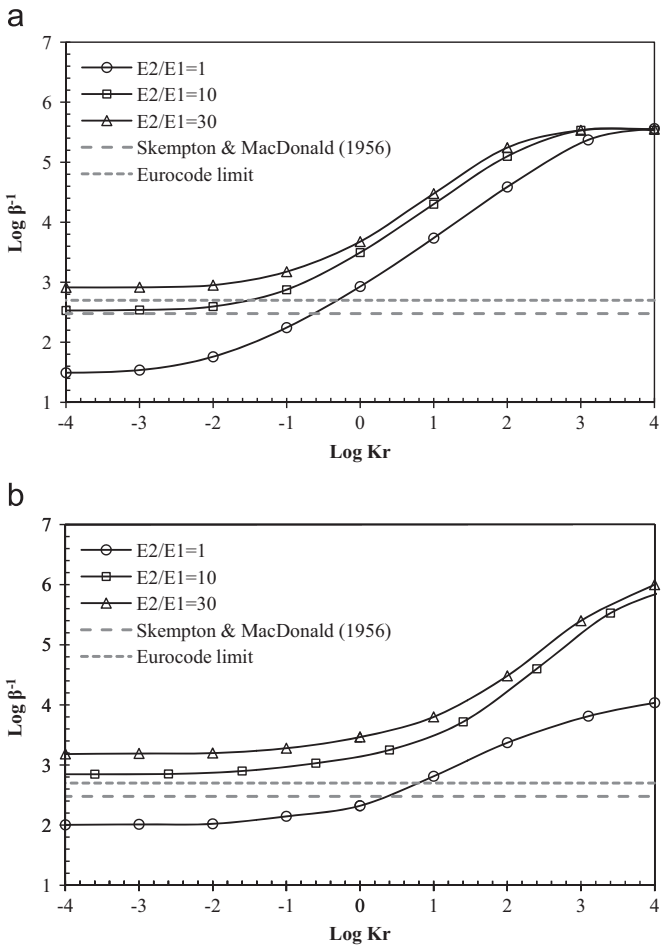

Fig. 20. (a) Influence of E_2/E_1 on β^{-1} for $N=9$. (b) Influence of E_2/E_1 on β^{-1} for $N=81$.

In the most generalised form, the supported superstructure may be idealised as a three-dimensional frame similar to that employed in a number of soil-foundation-structure studies reported in the literature, e.g., Cai et al. (2000) and Dutta and Roy (2002) (see Fig. 21). The framed structure is composed of three-noded line (beam) elements. The cross-sectional dimensions of the beams and girders were arbitrarily chosen as 0.3 m × 0.3 m, respectively, with a (concrete) Young's modulus of 30 GPa. The height of the columns was chosen as 2.5 m representing the typical height of 1 storey where n is the number of storeys. An illustration of the frame in the model is provided in Fig. 21 for an $N=9$ group.

Fig. 22 presents the results of the variation in β^{-1} with log K_r for n ranging between 0 and 5. The additional rigidity of the superstructure improves the angular rigidity of the group which supports the findings of Rethati (1961). It is clear that the additional rigidity provided by the supported superstructure should be taken into account for further optimisation of the pile cap design. It is noticeable, however, that the effect of n on

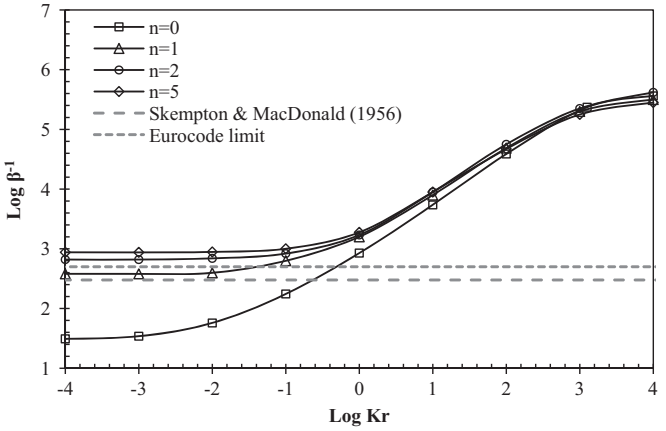

Fig. 22. Influence of supported structure on β^{-1}; $N=9$.

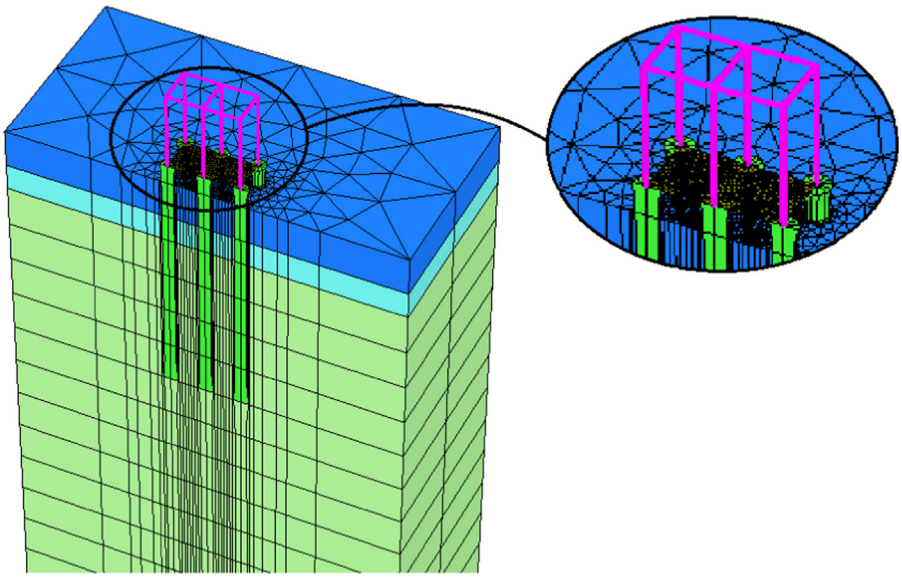

Fig. 21. Illustration of $n=1$ frame in FE model (half-symmetry) for $N=9$.

Table 2
Summary of parametric study.

Pile/soil parameter	Min	Max	Influence on EC7 β^{-1}
Constitutive model	LE	Nonlinear	↑↑↑
Cap–soil interaction	No	Yes	↑
B/s	0	0.5	↑↑↑
Soil type	Belfast	BBC	↑
FS	2.35	1.35	↑↑
N	3^2	9^2	↑↑↑
s/D	2	5	↑↑
m/n	1	9	↑
L/D	20	50	↑
E_2/E_1	1	30	↑↑↑
n (height)	0 (0)	5 (12.5 m)	↑↑↑

↑: $\Delta \log K_r < 0.5$, ↑↑: $0.5 < \Delta \log K_r < 1$, ↑↑↑: $\Delta \log K_r > 1$.

β^{-1} decreases with an increasing n over the range of interest, i.e., $|\log K_r| \leq 2$.

4.9. Group optimisation

A common feature of the aforementioned studies on the differential settlement of piled rafts was the consideration of the 'optimised' design. The aim of these optimised designs was to reduce the differential settlement, but they did not consider angular distortion/rigidity. The parametric analyses presented herein identified a number of variables that have the effect of increasing angular rigidity. Table 2 presents the parameters, and their respective ranges, considered in the previous parametric analyses. In addition, the authors have also attempted to summarise the relative influence of each pile/soil parameter on β^{-1} by documenting their effect on the value of log K_r corresponding to the Eurocode limit (EC7), which is of most interest. The authors have used an "arrow" system for this purpose, although it is recognised that the influence of each parameter depends on the ranges that were arbitrarily chosen.

For a pre-determined building footprint, it is clear that it is more advantageous to use a fewer number of piles, but longer piles. Reducing the number of piles benefits angular rigidity two-fold in that the pile-to-pile spacing may also then be increased. The study also identified the effectiveness of founding a pile group on a stiff stratum. If these are not sufficient (or feasible), the authors have investigated the effect of reducing the length of the outer perimeter of the piles, since the lowest values for β^{-1} occurred near the corner pile in most cases. This is shown in Fig. 23 where L_o is the length of the outer perimeter of the piles. The distribution of β^{-1} for a standard group (i.e., $L_o/L=1$) has been compared to that within an optimised group with values of L_o/L between 0.5 and 0.75, shown in Fig. 24, where the value for log $K_r=0$ was chosen arbitrarily. The load applied to the optimised groups was adjusted in order to maintain the same average FS per pile within the groups. It is clear that reducing the length of the piles in the outer ring is also effective for increasing β^{-1} within the groups.

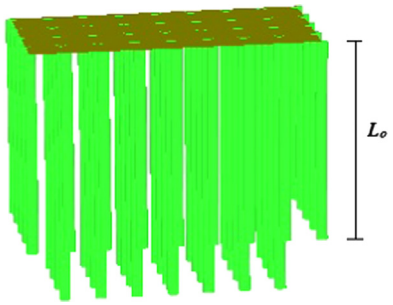

Fig. 23. Illustration of group with $L_o/L=0.75$.

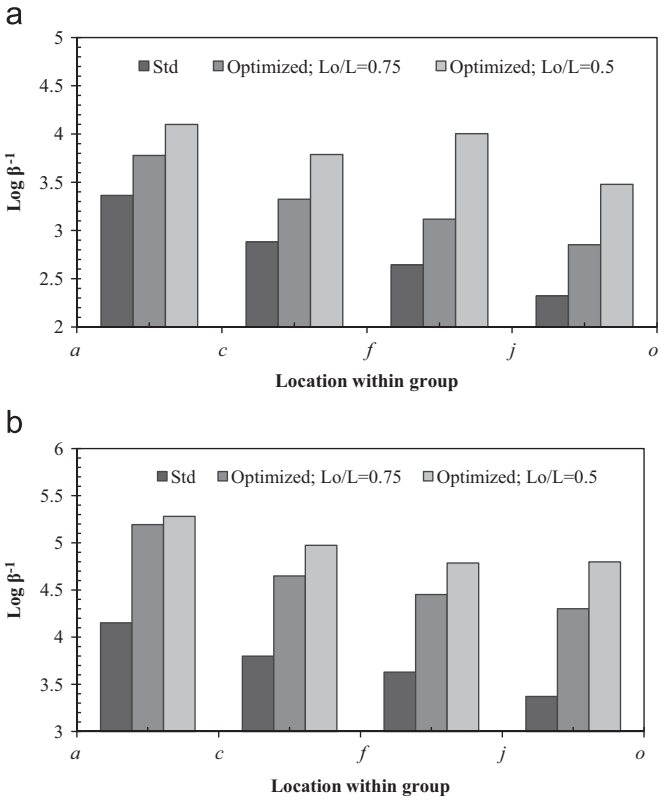

Fig. 24. (a) Influence of L_o/L on β^{-1} distribution in optimised groups; $N=81$, log $K_r=0$. (b) Influence of L_o/L on β^{-1} distribution in optimised groups; $N=81$, log $K_r=2$.

5. Comparison to measured data

5.1. Databases

For the purpose of putting some practical context on the predictions of differential group settlements using the present model, the previously presented PLAXIS results have been compared to three databases documented in the literature. The databases compiled by Skempton and MacDonald (1956), and later extended with additional information by Grant et al. (1974), documented the measured settlement characteristics of buildings. Those databases consisted of both isolated footings and rafts in clay; data in sand has also been included by way of comparison. The third database consisted of that compiled by

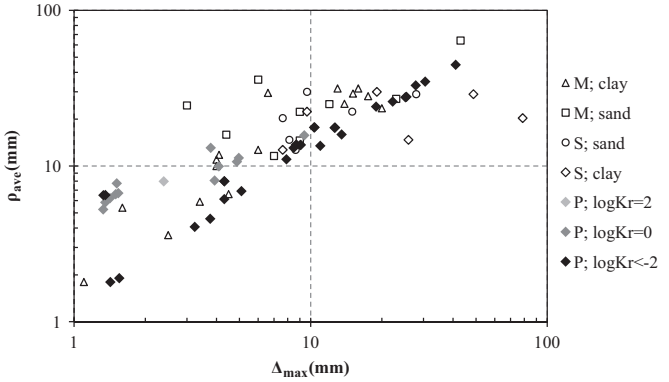

Fig. 25. Comparison of numerical results with field data for ρ_{ave} Vs Δ_{max}. M: Mandolini et al. (2005); S: Skempton and MacDonald (1956); P: *PLAXIS results*.

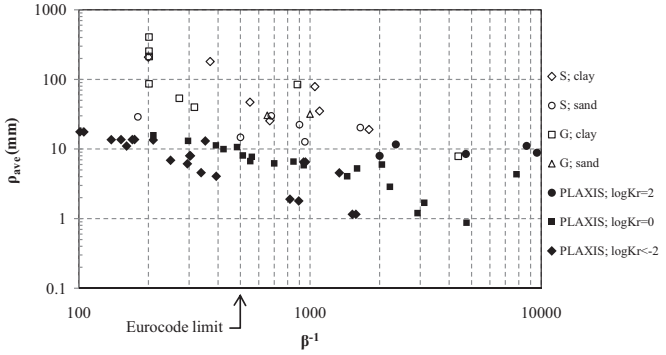

Fig. 26. Comparison of numerical results with field data for ρ_{ave} Vs β^{-1}. G: additional data documented by Grant et al. (1974).

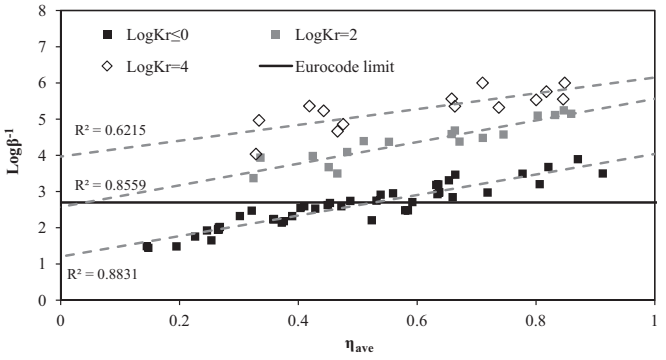

Fig. 27. Variation in β^{-1} with η_{ave} re-plotted.

Mandolini et al. (2005) for the settlement characteristics of a number of large-scale pile foundation case histories. Those foundations ranged in size from 4-pile to as large as 6,000-pile groups. The PLAXIS data presented in this section was derived from the parametric studies in the preceding sections. Table 2 documents the range in variables present in the PLAXIS data used in the following sections.

5.2. Maximum differential settlements

Maximum differential settlements have been the subject of a number of numerical studies (associated with piled rafts) and have also been featured in all three of the aforementioned databases. In Fig. 25, PLAXIS results have been compared to measured field data where the average settlement of the foundation, ρ_{ave}, is plotted against the maximum differential settlement of the foundation, Δ_{max}. In this study, ρ_{ave} is calculated according to Reul and Randolph (2004) as

$$\rho_{ave} = (2\rho_{centre} + \rho_{corner})/3 \quad (6)$$

where ρ_{centre} and ρ_{corner} are the settlements at the centre and the corner of the pile cap, respectively. In general, the output from PLAXIS appears to agree well with the measured data presented in the figure. Moreover, there appears to be a relatively linear trend in the relationship between the two measures of settlement.

5.3. Angular distortion

Grant et al. (1974) presented a relationship between ρ_{ave} and β which has been compared to PLAXIS data in Fig. 26. Both the numerical and the measured data show similar trends and a reasonable agreement is evident. The authors attribute the lack of exactness in the agreement between the measured and the numerical data to:

- The measure for the overall foundation settlement (ρ_{ave}) is not normalised, and thus, is influenced by the range of pile/soil parameters and
- The conservatism inherent in the numerical data arises from the parameters that formed the basis of the parametric study discussed in Section 3.

6. Fully normalised trends from numerical results

The authors have extended the results presented in the previous case to the case of fully normalised trends (i.e., η_{ave} versus β^{-1}), since η and β^{-1} are superior measures of the pile foundation settlement performance.

In Fig. 27, the variation in β^{-1} with η_{ave}, determined using the PLAXIS output, has been plotted for a range in values of log K_r for Belfast clay with $B/s=0$ and FS = 1.35. Therefore, only the variation in geometric parameters was considered in these plots, allowing a like-with-like comparison. Best fit lines through the data have also been superimposed in the figure for each value of log K_r where log $K_r \leq 0$ data have been combined because they showed a good agreement. The limit set down in Eurocode 7 has also been superimposed in the figure. It can be seen that a value of at least log $K_r = 0$ is required to maintain the level of angular rigidity above the Eurocode limit. The findings presented in Fig. 27, which include the results with a variation in n from 0 to 5, support the study by Grant et al. (1974) who documented that the number of storeys had an insignificant influence on the relationships between angular distortion and settlement performance. Values for R^2 of 0.88 for log $K_r \leq 0$ indicate strong evidence of a

relationship between foundation stiffness efficiency and angular rigidity.

In order to obtain an estimate for β^{-1} for a pile group foundation, the trends presented in Fig. 27 can be used in conjunction with an approach capable of obtaining an estimate for η_{ave} for the group. The simplified finite element-based approach, documented by Sheil and McCabe (2014), was developed using a similar framework to the present study and is a compatible way to estimate η_{ave}.

7. Conclusions

A numerical study of angular rigidity has been presented in this paper using the Hardening Soil (HS) model in the PLAXIS 3-D Foundation finite element (FE) software package. A number of consistent trends were featured in the study, thus allowing the following conclusions to be drawn.

(a) The majority of studies on the subject of differential pile foundation settlement to date have considered overall differential settlements. Reports on damage to buildings, however, have identified angular distortion, β, as the most influential settlement characteristic in the serviceability of supported superstructures.
(b) A number of studies have attempted to reinforce the continued use of LE analyses in appropriate situations, such as for 'interactive' pile displacements. However, this study has shown that stress-dependent soil stiffness has an important influence on predictions of angular rigidity, β^{-1}, when the group is modelled as a continuum; LE analyses provide non-conservative predictions.
(c) A parametric study has been undertaken in which a number of pile/soil parameters were varied in order to identify their relative influence on β^{-1}. The influence of the respective variables was qualitatively summarised by the authors following the parametric analyses.
(d) Pile foundations may be optimised for angular rigidity when reducing the length of the outer perimeter of the piles is shown to be very effective in increasing the distribution of angular rigidity within the group.
(e) Obvious trends between group settlement performance (i.e., average stiffness efficiency) and angular rigidity have been documented, thus providing design engineers with a practical resource for the estimation of pile foundation angular distortion.

Acknowledgements

The first author is grateful for the support of the College of Engineering and Informatics Fellowship awarded by the National University of Ireland, Galway, Ireland.

References

Brown, P.T., 1975. The significance of structure–foundation interaction. In: Proceedings of the 2nd Australia–New Zealand Conference on Geomechanics, IEQust, Brisbane.
Cai, Y.X., Gould, P.L., Desai, C.S., 2000. Nonlinear analysis of 3D seismic interaction of soil–pile–structure systems and application. Eng. Struct. 22 (2), 191–199.
Cheung, Y.K., Tham, L.G., Guo, D.J., 1988. Analysis of pile group by infinite layer method. Geotechnique 38 (3), 415–431.
Cho, J., Lee, J.H., Jeong, S., Lee, J., 2012. The settlement behaviour of piled raft in clay soils. Ocean. Eng. 53, 153–163.
Dutta, S.C., Roy, R., 2002. A critical review on idealization and modeling for interaction among soil–foundation–structure system. Comput. Struct. 80 (20), 1579–1594.
Gavin, K.G., Igoe, D., Doherty, P., 2011. Use of open-ended piles to support offshore wind turbines: a state of the art review. Proc. ICE Geotech. Eng. 164 (GE4), 245–256.
Grant, R., Christian, J.T., Vanmarcke, E.H., 1974. Differential settlement of buildings. J. Geotech. Geoenviron. Eng. 100 (9), 973–991.
Guo, D.J., Tham, L.G., Cheung, Y.K., 1987. Infinite layer for the analysis of a single pile. Comput. Geotech. 3 (4), 229–249.
Horikoshi, K., Randolph, M.F., 1998. A contribution to the optimum design of piled rafts. Geotechnique 48 (2), 301–317.
Jappeli, 1965. Settlement studies of some structures in Europe. In: Proceedings of the 6th International Conference on Soil Mechanics and Foundation Engineering, pp. 88–92.
Leung, Y.F., Soga, K., Lehane, B.M., Klar, A., 2010. Role of linear elasticity in pile group analysis and load test interpretation.". J. Geotech. Geoenviron. Eng. 136 (12), 1686–1694.
Mandolini, A., Russo, G., Viggiani, C., 2005. Pile foundations: experimental investigations, analysis and design. Ground. Eng. 38 (9), 34–35.
McCabe, B.A., Lehane, B.M., 2006. Behavior of axially loaded pile groups driven in clayey silt. J. Geotech. Geoenviron. Eng. 132 (3), 401–410.
McCabe, B.A., Sheil, B.B., 2015. Pile group settlement estimation: suitability of nonlinear interaction factors. ASCE Int. J. Geomech. http://dxdoi.org/10.1061/(ASCE)GM.1943-5622.0000395 (in press).
Poulos, H.G., 1968. Analysis of the settlement of pile groups. Geotechnique 18 (4), 449–471.
Poulos, H.G., 2001. Piled-raft foundation: design and applications. Geotechnique 127 (1), 17–24.
Prakoso, W.A., Kulhawy, F.H., 2001. Contribution to piled raft foundation design. J. Geotech. Geoenviron. Eng. 127 (1), 17–24.
Rethati, 1961. Behaviour of building foundations on embankments. In: Proceedings of the 5th International Conference on Soil Mechanics and Foundation Engineering, p. 781.
Reul, O., Randolph, M.F., 2004. Design strategies for piled rafts subjected to nonuniform vertical loading. J. Geotech. Geoenviron. Eng. 130 (1), 1–13.
Sheil, B.B., McCabe, B.A., 2014. A finite element based approach for predictions of rigid pile group stiffness efficiency in clays. Acta Geotech. 9, 469–484.
Skempton, A.W., MacDonald, D.H., 1956. The allowable settlement of buildings. ICE Proc. Part III 5, 727–784.
Thorburn, S., Laird, C., Randolph, M.F., 1983. Storage tanks founded on soft soils reinforced with driven piles. In: Proceedings of the Conference of Recent Advances in Piling and Ground Treatment for Foundations, ICE, London, pp. 157–164.
Timoshenko, S., Woinowsky-Krieger, S., 1959. Theory of plates and shells. McGraw-Hill, New York.
Wahls, H.E., 1994. Tolerable deformations. Geotechnical Special Publication No. 40, ASCE, New York, pp. 1611–1628.
Zhang, L.M., Ng, A.M.Y., 2005. Probabilistic limiting tolerable displacements for serviceability limit state design of foundations. Géotechnique 55 (2), 151–161.